Charge movement in gating-locked HCN channels reveals weak coupling of voltage sensors and gate

Sujung Ryu and Gary Yellen

Department of Neurobiology, Harvard Medical School, Boston, MA 02115

HCN (hyperpolarization-activated cyclic nucleotide gated) pacemaker channels have an architecture similar to that of voltage-gated K^+ channels, but they open with the opposite voltage dependence. HCN channels use essentially the same positively charged voltage sensors and intracellular activation gates as K^+ channels, but apparently these two components are coupled differently. In this study, we examine the energetics of coupling between the voltage sensor and the pore by using cysteine mutant channels for which low concentrations of Cd^{2+} ions freeze the open–closed gating machinery but still allow the sensors to move. We were able to lock mutant channels either into open or into closed states by the application of Cd^{2+} and measure the effect on voltage sensor movement. Cd^{2+} did not immobilize the gating charge, as expected for strict coupling, but rather it produced shifts in the voltage dependence of voltage sensor charge movement, consistent with its effect of confining transitions to either closed or open states. From the magnitude of the Cd^{2+}-induced shifts, we estimate that each voltage sensor produces a roughly three- to sevenfold effect on the open–closed equilibrium, corresponding to a coupling energy of ~1.3–2 kT per sensor. Such coupling is not only opposite in sign to the coupling in K^+ channels, but also much weaker.

The Journal of General Physiology

INTRODUCTION

HCN (hyperpolarization-activated cyclic nucleotide gated) channels are widely expressed throughout the heart and the nervous system, including the sino-atrial node, hippocampal pyramidal cells, and photoreceptor cells (Kaupp and Seifert, 2001). They play a key role in regulating rhythmic activity of cardiac pacemaker cells and spontaneously firing neurons (McCormick and Pape, 1990; DiFrancesco, 1993). They are also involved in various neuronal processes, including dendritic integration (Magee, 1999), synaptic transmission (Beaumont et al., 2002), and the temporal processing of visual signals in the retina (Demontis et al., 1999). Four mammalian HCN channel subunits (mHCN 1–4) have been found so far (Santoro et al., 1997, 1998; Ludwig et al., 1998; Ishii et al., 1999), and homologues have been cloned from several invertebrates such as sea urchins (SPIH or sea urchin HCN [spHCN]; Gauss et al., 1998) and bacteria (Sesti et al., 2003). The functional loss of HCN channels leads to defects in the learning of motor tasks or to serious cardiovascular conditions such as arrhythmia, congestive heart failure, or myocardial infarction (Biel et al., 2009).

HCN channels are structurally similar to voltage-gated K^+ channels in that they have six transmembrane segments (S1–S6) that include a putative voltage sensor (S4) and a pore region between S5 and S6 (Kaupp and Seifert, 2001). Moreover, the S4 movement in the spHCN channels is similar to that in voltage-gated Kv channels such as *Shaker* channels (Männikkö et al., 2002). However, unlike typical voltage-gated K^+ channels that are gated by depolarization, HCN channels are activated by hyperpolarization. Using the same intracellular gate, inward movement of the voltage sensor upon hyperpolarization is coupled to channel opening in HCN channels (Männikkö et al., 2002; Rothberg et al., 2002). The coupling mechanism in spHCN channels is also peculiar in that the inward movement of the voltage sensors may be loosely coupled to channel opening when cAMP is absent, allowing the gates to slip back to the closed state (inactivation, desensitization to voltage, or loss of coupling; Shin et al., 2004). The binding of cAMP to the C-terminal cyclic nucleotide–binding domains can relieve this fast inactivation process and increase the maximum open probability.

The domains of HCN channels that are important for voltage gating have been identified from previous studies (Chen et al., 2001; Männikkö et al., 2002; Bell et al., 2004). Alanine-scanning mutagenesis indicates the S4–S5 linker is involved in the coupling between S4 movement and channel gating (Chen et al., 2001), but the details of the mechanism that couples the voltage sensors to gating are still not fully understood. Several kinetic models have been suggested to explain the molecular basis of voltage-dependent gating in HCN channels (Altomare et al., 2001; Wang et al., 2002; Shin et al., 2004; Männikkö et al., 2005). However, information

Correspondence to Gary Yellen: gary_yellen@hms.harvard.edu

The Rockefeller University Press $30.00
J. Gen. Physiol. Vol. 140 No. 5 469–479
www.jgp.org/cgi/doi/10.1085/jgp.201210850

about the energetics and mechanism of voltage-gated opening in HCN channels is still sparse.

Previous studies found that cysteine substitutions at positions H462 and L466 in the S6 region of the spHCN channel produce a "locked-open" phenotype of the channel when Cd^{2+} is applied to the cytosolic side of the channels, apparently because the Cd^{2+} ion can form an energetically favorable bridge between the two cysteines (Rothberg et al., 2003). A comparable "locked-closed" phenotype with Cd^{2+} application is seen for the Q468C mutant (studied in the presence of an H462Y mutation to prevent a competing locked-open effect; Rothberg et al., 2003). Here, we exploited the effects of Cd^{2+} on these mutants to study the coupling energetics between voltage sensor and channel gating by measuring gating currents of the locked-open and locked-closed mutants expressed in *Xenopus laevis* oocytes. We found that Cd^{2+} shifted the gating charge-voltage (Q-V) relationship to more positive potentials for a locked-open mutant (462C466C), whereas it shifted the Q-V relationship to more negative potentials for a locked-closed mutant (462Y468C). We used these data together with a simple allosteric model for coupling between the voltage sensors and the opening/closing transitions to describe the coupling energetics of these hyperpolarization-activated channels.

MATERIALS AND METHODS

Expression of recombinant HCN channels

cDNA for wild-type spHCN channels was transcribed in vitro using T7 RNA polymerase (mMessage Machine; Invitrogen). The final cRNA was resuspended in RNase-free water to a final concentration of 1 µg/µl and kept at −80°C. Defolliculated *Xenopus* oocytes were prepared and injected with ∼30–50 nl cRNA. Injected oocytes were incubated at 16–20°C in ND96 (96 mM NaCl, 5 mM KCl, 1 mM $MgCl_2$, 1.8 mM $CaCl_2$, and 5 mM HEPES, pH 7.6) supplemented with 5 mM sodium pyruvate and 5 mg/100 ml gentamicin and used for electrophysiological recordings after 1–3 d.

Solutions and electrophysiological recordings

All experiments for measuring gating currents were performed with giant inside-out patches (Hilgemann, 1989), and experiments for ionic currents were performed with inside-out patches. Patch pipettes with a resistance of 180–250 kΩ were pulled in two stages, and their tips were made hydrophobic by coating them with a mixture of mineral oil and wax for giant patch recordings. Patch pipettes of ∼1-MΩ resistance were prepared for inside-out patch recordings. Data were acquired using an amplifier (Axopatch 200B; Molecular Devices) that was low-pass filtered at 5–10 kHz and digitized at 25 kHz. pClamp 8 software (Axon Instruments) was used for amplifier control and data acquisition. All experiments were performed at room temperature (22–24°C).

For giant inside-out patch recordings, the bath and pipette solutions contained the following (mM): 160 NMDG, 160 $MeSO_3$, 0.5 Mg^{2+}, 2 Cl^-, 1 nitrilotriacetic acid, and 10 HEPES (pH 7.4 with NMDG). For inside-out patch recordings, the bath solution contained (mM) 140 KCl, 1 EGTA, 0.5 $MgCl_2$, and 10 HEPES (pH 7.4 with KOH), and the pipette solution contained (in mM) 140 KCl, 0.5 $MgCl_2$, and 10 HEPES (pH 7.4 with KOH). All chemicals were purchased from Sigma-Aldrich. For all experiments, the intracellular solution also contained 100 µM cAMP, which saturates the cAMP binding site and eliminates the inactivation process seen for spHCN channels in the absence of cAMP.

Methods for rapid perfusion were performed as described previously (Liu et al., 1997). The solution exchange time (∼1 ms) was determined at the end of experiments by examining the current response for an open patch pipette during a switch to a 160 mM K^+ solution.

Data analysis

Conductance-voltage (G-V) curves were obtained from the amplitude of the tail currents at 60 mV. The conductance-voltage (G-V) and Q-V curves were fitted with Origin 7 (OriginLab) using the Levenberg-Marquardt algorithm and the instrumental weighting method. A Boltzmann equation ($Q = 1/(1+\exp[(V - V_{1/2})zF/RT)]$) was used to fit the Q-V curve to estimate the $V_{1/2}$ (the voltage at which half of the charge is transferred) and z (the valence of the transferred charge). Linear capacitive currents were subtracted by a −P/4 protocol from a secondary holding potential of 60 mV. Gating charge moved during each test hyperpolarization (Q_{ON}) was quantified by integrating the first 50ms of gating currents during hyperpolarization (Q_{ON}) or depolarization (Q_{OFF}), after defining the baseline to be the steady-state current level for at least the last 5ms.

For the fitting of Q-V and G-V curves using a 10-state MWC (Monod-Wyman-Changeux) allosteric model (see Fig. 1 A), the following equilibrium equations were used:

$$\frac{Q}{Q_{\max}} = \frac{J(1+J)^3 + L\cdot J\cdot\theta(1+J\cdot\theta)^3}{(1+J)^4 + L(1+J\cdot\theta)^4} \text{ and}$$

$$\frac{P}{P_{\max}} = \frac{J(1+J\cdot\theta)^4}{(1+J)^4 + L(1+J\cdot\theta)^4},$$

where L is the equilibrium constant for the C-O transition when the voltage sensor is in the deactivated state, and $J = J_0 \exp(-zV/kT)$, where J_0 is the equilibrium constant for the activation of a single voltage sensor when the channel gate is closed. θ is the coupling factor between voltage sensor activation and channel gating, and z is the effective gating charge for a single sensor. Model parameters were estimated from a simultaneous fit to the Q-V curves (with and without Cd^{2+}) and the G-V curve (obtained from rapid perfusion, as in Fig. 2). Parameter error estimates were those obtained from the nonlinear fit in Origin 7, using nominal instrumental errors of 0.05 (on a scale from zero to one) rather than the observed errors in order to avoid distortions caused by the low errors for points near zero and one produced by the normalization procedure.

Online supplemental material

Fig. S1 shows Q-V curves for wild-type spHCN channels in the absence and presence of intracellular Cd^{2+}, illustrating the lack of effect. Fig. S2 shows the G-V relations for wild-type spHCN, 462C466C, and 462Y468C, measured with activating voltage steps applied in symmetrical NMG-containing solutions, but with tail currents measured immediately after rapid perfusion of K^+-containing solution to the exposed (intracellular) face of the patch. Online supplemental material is available at http://www.jgp.org/cgi/content/full/jgp.201210850/DC1.

RESULTS

Approaches to estimating the coupling between voltage sensor activation and channel opening

The relationship between voltage sensor activation and channel opening of the spHCN channel can be illustrated

by a gating scheme based on a standard MWC allosteric model, as previously used for voltage-gated channels such as BK Ca^{2+}-activated K^+ channels (Monod et al., 1965; Cox et al., 1997). Because spHCN channels contain four voltage sensors (Biel et al., 2009), the model results in a scheme with 10 states, comprising open and closed states with varying numbers (zero to four) of activated voltage sensors (Fig. 1 A). According to this voltage-dependent MWC scheme (Fig. 1 A), the closed (C)–open (O) equilibrium constant, which governs transitions between a closed state at the top of the diagram and an open state at the bottom, will vary with the number of activated voltage sensors (left-right transitions): when voltage sensors are in the deactivated state, gating equilibrium is biased toward the closed state, whereas when voltage sensors are in the activated state, the gating equilibrium is biased toward the open state. It necessarily follows from the energetics of the system that the state of the gate (open or closed) will affect the tendency of voltage sensors to activate; in open channels, voltage sensors can activate more easily (in the diagram, this corresponds to horizontal state changes). This allosteric linkage between channel opening and voltage activation, quantified by coupling factor θ, accounts for the ability of voltage sensors to affect open probability or vice versa.

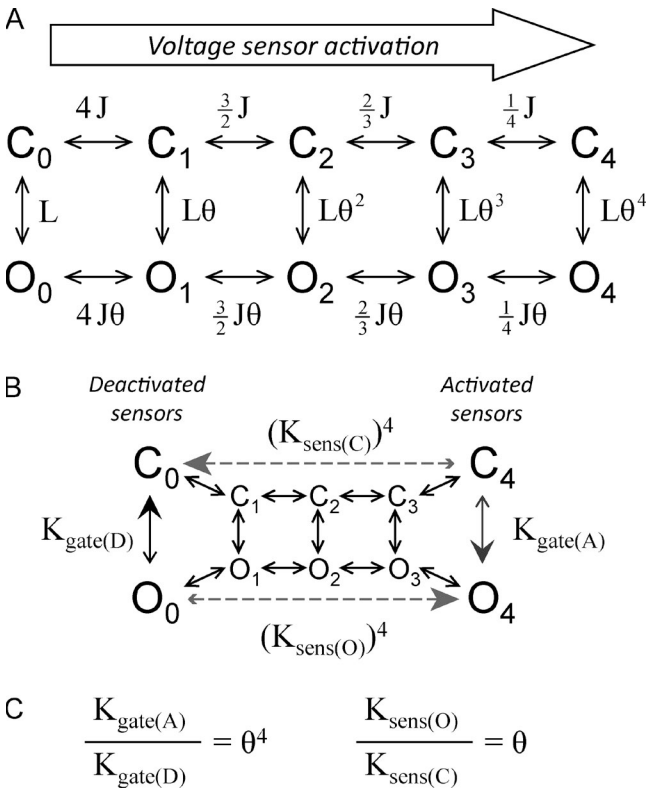

Figure 1. Equilibrium models of coupling between voltage sensors and gating. (A) Standard allosteric model for coupling of four voltage sensors to simple channel opening. (B) Simplified version of A, with equilibrium constants summarized for fully activated (A) and deactivated (D) voltage sensors and open (O) and closed (C) channels. The diagram is heuristic and does not indicate a direct connection between C_0 and C_4 or between O_0 and O_4; the overall equilibrium constants shown between these extreme states are simply equal to the product of the intervening equilibrium constants. (C) Two approaches to estimating the coupling constant θ.

The focus of our study is to measure this coupling factor, which reveals the energetics of coupling between the voltage sensor and the channel gating in spHCN channels. Conceptually, the coupling factor (θ) describes the ratio of equilibrium constants, either for gating in various states of the sensor or for the sensor in various gating states. A conceptually simpler diagram can be used to emphasize the energetics between the limiting (fully activated or fully deactivated, open or closed) states of the channel (Fig. 1 B). In the context of this simplified diagram, we also show an alternative (but equivalent) description of the equilibrium constants: $K_{gate(D)}$ and $K_{gate(A)}$ are the equilibrium constants for the far left and far right vertical transitions, and they describe the open–closed equilibrium constants for fully deactivated versus activated sensors. $K_{sens(C)}$ and $K_{sens(O)}$ are the equilibrium constants for the activation of a single voltage sensor when the channel gate is either closed or open. In this framework, there are two ways to measure the coupling factor θ (Fig. 1 C): either by measuring the ratio of closed–open equilibrium constants for the activated and deactivated positions of the voltage sensors or the ratio of the equilibrium constants for gating charge movement with the channel in the open state versus in the closed state (Fig. 1 C).

The first way of calculating θ, using the open–closed equilibrium constants at extreme voltages, is error prone: the equilibrium constants are hard to calculate precisely when open probability is close to 0 or close to 1. Although single-channel currents through spHCN channels have been recorded successfully in a previous study (Dekker and Yellen, 2006), it is difficult to measure the open probabilities at extreme voltage conditions using single-channel recordings. Even if successful, this approach would be likely to give an erroneous estimate of the magnitude of the closed–open equilibrium constants that are coupled to the sensors. At maximum activating voltages, ion channels rarely have an open probability of 1 because of fast flicker gating and ionic block of the channel. At deactivating voltages, spHCN channels exhibit a voltage-independent opening process (Proenza and Yellen, 2006) that would obscure the limiting voltage-dependent equilibrium constant for gating.

These problems suggest the use of the alternative way of calculating θ, by measuring the voltage sensor equilibrium when the channel is always closed or always open. Because this ratio is θ rather than θ^4, the expected changes are less extreme, and because the equilibrium is measured by varying voltages and examining the midpoints, the changes are more measureable. The locked-open and locked-closed effects of Cd^{2+} that we have

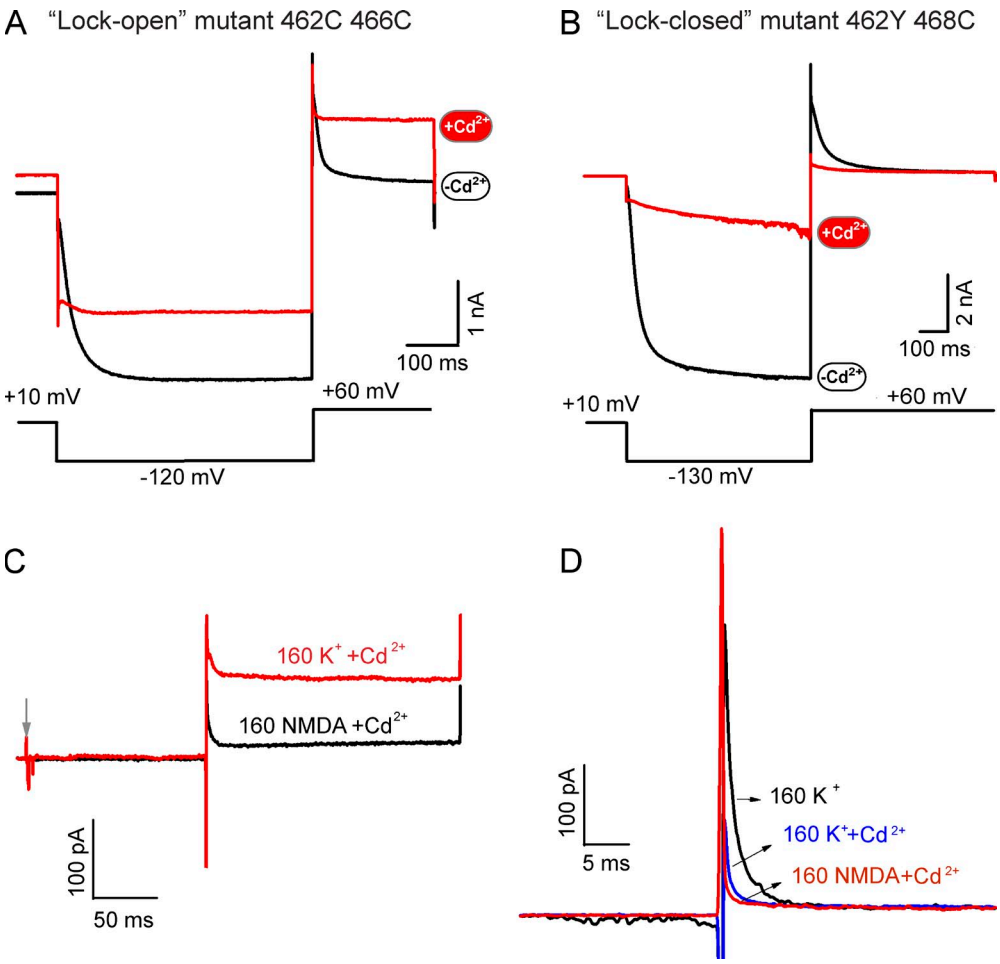

Figure 2. Effect of Cd^{2+} on the 462C466C mutant or 462Y468C mutant. (A and B) Representative recordings from inside-out patches excised from *Xenopus* oocytes expressing either spHCN 462C466C (A) or spHCN 462Y468C (B) before and during the application of 130 nM free Cd^{2+}. Channels were held at 10 mV, and currents were elicited by a step to −120 (A) or −130 mV (B), followed by a step to 60 mV. Currents were not leak subtracted. (C and D) To test whether the expressed channels still represent mutant phenotype in the condition of measuring the gating current (160 mM NMDA + 160 mM $MeSO_3$ for pipette and bath), a 160 mM K^+ solution was applied rapidly to inside-out patches expressing spHCN 462C466C (C) or spHCN 462Y468C (D). The black trace in C indicates the response with NMDA on both sides and 130 nM free Cd^{2+}, whereas the red trace shows the current response with the switch to intracellular K^+ immediately before the voltage step from −120 to 60 mV; the sustained outward current indicates the locked-open effect. The gray arrow in C indicates the time when the solenoid was engaged; the solution switch at the patch occurred ∼50 ms later, and the actual switching speed was <1 ms. (D) The black trace shows a normal tail current for the locked-closed mutant in the absence of Cd^{2+} when intracellular K^+ was applied immediately before the voltage step from −120 to 60 mV. The red trace again shows the response with fast perfusion of K^+ solution, but in the constant presence of 130 nM free Cd^{2+}, and the blue trace indicates the gating current alone (no K^+ perfusion) with 130 nM free Cd^{2+} present.

observed for certain cysteine mutant channels offer an opportunity for measuring K_{sens} when the channels are confined to only open states or only closed states.

However, neither mutant permits a direct comparison between K_{sens} for fully open and fully closed channels; for each mutant, in the absence of Cd^{2+}, the voltage sensor equilibrium constant represents a mix of open and closed channels, whereas in the presence of Cd^{2+}, we can measure a relatively pure open or closed equilibrium.

Cd^{2+}-induced effects on mutant gating persist under gating current conditions

We have previously found that spHCN channels with cysteine substitutions at positions 462 and 466 in the S6 region can be locked open by low concentrations of Cd^{2+} applied to the cytosolic side of the channels (Rothberg et al., 2003). As shown in Fig. 2 A, the normal closing of the channels at positive voltages (black trace), apparent as a time-dependent tail current, is nearly abolished with the application of Cd^{2+} (red trace); the lock-open effect is also apparent by the large inward current immediately after the hyperpolarizing step. In contrast, channels with 462Y468C mutations in S6 exhibit a locked-closed effect with 130 nM free Cd^{2+}, which is apparent as an extreme slowing of the activation at negative voltages (Fig. 2 B, red trace), with the degree of slowing dependent on $[Cd^{2+}]$ (Rothberg et al., 2003). Because the Cd^{2+} binding is reversible, the locked-closed effect is not permanent—the small fraction of channels without Cd^{2+} bound will open (and no longer bind Cd^{2+} because of movement of the cysteines); this results in a very slow increase in current over time during hyperpolarization (Rothberg et al., 2003).

Before we tested the effect of Cd^{2+} on the gating current in these mutants (462C466C and 462Y468C), we examined whether the mutants still retained their phenotypic characteristics of either locked open or locked closed under the very different ionic conditions used for measuring gating current. We typically measured gating currents in inside-out patches under conditions

in which no ionic current flows through the channel by using nonconducting NMDG-methanesulfonate instead of K^+. To test the actual state of the channel gates during the gating current measurement, we quickly changed the solution from nonconducting conditions (i.e., NMDG-methanesulfonate solution) to ionic current conditions (i.e., 160 mM K^+) using a rapid perfusion system. These experiments were performed in the constant presence of a saturating concentration of Cd^{2+} (130 nM free Cd^{2+}).

In gating current conditions with no K^+ present, we held the membrane voltage at 60 mV, applied an opening pulse to –120 mV, and then depolarized back to 60 mV. The return of voltage sensors upon the final depolarization (seen from the OFF gating current, $I_{g,OFF}$) of 462C466C was rapid (Fig. 2 C, black trace). When 160 mM K^+ was applied rapidly just before the depolarization to 60 mV, the subsequent ionic tail current showed the typical locked-open phenotype of extremely slow and incomplete deactivation, as shown in Fig. 2 C (red trace). This result shows that channels were open and stabilized by Cd^{2+} even under gating current conditions, before the rapid reapplication of K^+. The 462Y468C mutant also showed its characteristic (but opposite) behavior in Cd^{2+}: the patch was switched rapidly into K^+-containing solution at the end of the activating pulse, and the subsequent depolarizing pulse showed no ionic tail current, consistent with Cd^{2+} maintaining the channels in a closed state even during the activating voltage in nonconducting conditions (Fig. 2 D).

Locking channels open makes it easier to activate their voltage sensors

To elucidate the energetic contribution of voltage sensor activation to channel gating, we measured how locking channels open with Cd^{2+} affected the voltage dependence of gating currents. We first measured control gating currents in wild-type spHCN channels. Cd^{2+} application to the cytosolic side did not change the gating charge movement of the wild-type channels significantly compared with the absence of Cd^{2+} (Fig. S1), as previously seen for G-V curves of wild-type spHCN (Rothberg et al., 2002).

We next tested for changes in gating charge movement when the 462C466C mutant channel was locked open by Cd^{2+} (Fig. 3). Application of Cd^{2+} to this locked-open mutant right shifted the Q-V curve by 20 mV, indicating that locking the gate in the open state favors the activated state of the voltage sensors but does not immobilize them as seen when *Shaker* channels are locked open by N-type inactivation (Bezanilla et al., 1991). Because Cd^{2+} locks most of the channel gates in the open state, the OFF gating current represents a relatively pure measurement of $K_{sens(O)}$, the voltage-dependent equilibrium constant for voltage sensor movement in the open channel, as diagrammed in Fig. 3 A. The Q_{OFF}-V shift to more positive potentials with Cd^{2+} in the locked-open mutant (Fig. 3 E) implies that the movement of voltage sensors while the channels are fixed in the open state is more favorable compared with the closed state (or, rather, compared with the mixture of closed- and open-state charge movements obtained in the absence of Cd^{2+}). A similar shift was seen for the ON gating charge movement (Q_{ON}-V; Fig. 3 D), and the magnitude of this shift provides information about the energetic coupling.

Locking channels closed makes it more difficult to activate their voltage sensors

For the 462Y468C locked-closed mutant, the channels can be held in the closed state by the application of Cd^{2+}, as shown in Fig. 4 A. The Q_{OFF}-V in the presence of Cd^{2+} was negatively shifted (by approximately −20 mV) compared with the Q-V in the absence of Cd^{2+}, indicating that stabilization of the closed state biases the voltage sensors toward the deactivated state, such that more hyperpolarization is required to activate them (Fig. 4 E). The Q_{ON}-V curve was also left shifted by ∼20 mV (Fig. 4 D). The maximal ON gating charge appeared to be reduced ∼10% by Cd^{2+} application, but when we increased the time interval for measuring ON gating current from 100 to 300 ms, the total Q_{ON} with or without Cd^{2+} became indistinguishable (unpublished data); this suggests that the change in the apparent total Q_{ON} for the shorter pulse occurred only because ON gating charge becomes slower with the application of Cd^{2+}. Cd^{2+} produced no change in the Q-V curve for control spHCN channels without the introduced cysteines (unpublished data), arguing that the changes were not caused by nonspecific effects of Cd^{2+} on the channel or the electric field.

DISCUSSION

We have measured gating currents of two spHCN mutant channels (462C466C and 462Y468C), exploiting the effect of Cd^{2+} on these mutants to examine subsets of the voltage activation process in isolation. When we used Cd^{2+} to lock these channels in either the closed or the open state, we found that a voltage-dependent gating current (representing movement of the voltage sensors) could nevertheless be measured. Were the coupling between voltage sensors and gate very strict, as it is, for instance, in *Shaker* K^+ channels, we would have expected immobilization of the gating charge when channels are locked open or closed. Instead, locking the 462C466C mutant channels open with Cd^{2+} caused charge movement to occur at more positive voltages (a shift of ∼20 mV), consistent with an easier activation of the voltage sensors when the gate is in the open state. On the other hand, Cd^{2+} shifted the Q-V curves of the 462Y468C mutant to more negative voltages, consistent with more difficult activation of voltage sensors when the gate is closed.

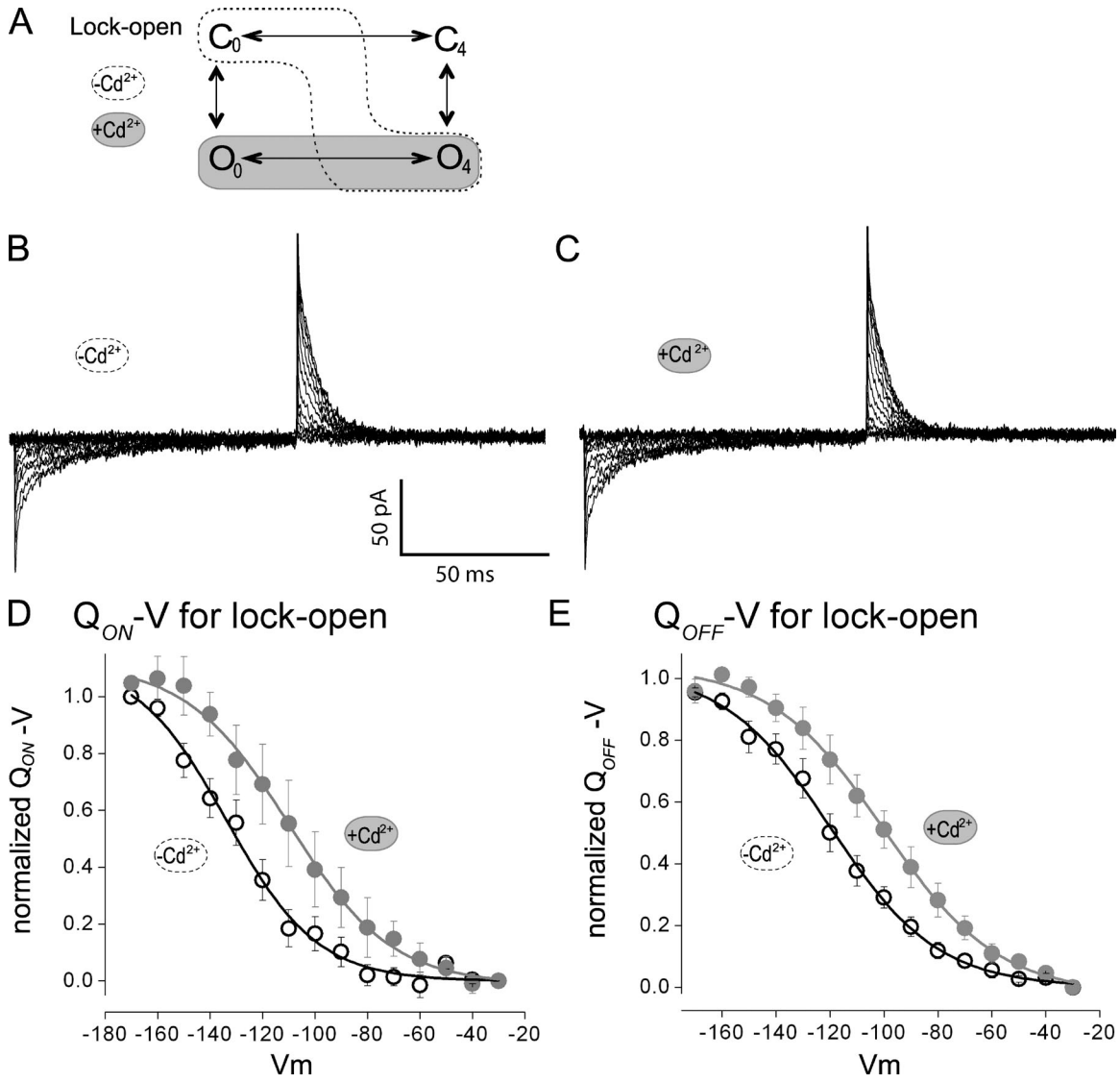

Figure 3. Gating current and Q-V relations for the spHCN 462C466C mutant. (A) Schematic description of the locked-open mutant. The state of the channel with Cd^{2+} is shaded, whereas the control condition without Cd^{2+} is in the dashed area. (B and C) Traces of gating current records for spHCN 462C466C without (B) or with 130 nM free Cd^{2+} (C), from the same patch. Holding potential was 10 mV, and test pulses were from −30 to −170 mV in 10-mV increments. A −P/4 protocol was used to subtract leak and linear capacitive currents. (D and E) Normalized Q-V relations for spHCN 462C466C without Cd^{2+} (open circles) or with Cd^{2+} (closed circles). Both Q_{ON} (D) and Q_{OFF} (E) were obtained by integrating components. Smooth curves are single Boltzmann fits to the data with these parameters: Q_{ON} control: $V_{1/2}$ = −132.7 ± 2.1 mV, slope factor (e-fold) = 16.5 ± 1.2; Cd^{2+}: $V_{1/2}$ = −103.9 ± 5.3 mV, slope factor (e-fold) = 18.2 ± 1.2; n = 5. Q_{OFF} control: $V_{1/2}$ = −126.7 ± 5.1 mV, slope factor (e-fold) = 21.1 ± 1.2; Cd^{2+}: $V_{1/2}$ = −99.9 ± 5.3 mV, slope factor (e-fold) = 19.5 ± 1.1; n = 9. Error bars represent SEM.

These Q-V shifts seem most likely to result from conformational stabilization by the Cd^{2+} ion bridging the introduced cysteines. No effects were seen on the Q-V for control channels lacking these cysteines. Also, as the bound Cd^{2+} displaces the sulfhydryl protons, there should be zero net charge on the –S–Cd–S– complex, arguing against a simple electrostatic effect of bound Cd^{2+} on the voltage sensors unrelated to its conformational effects.

The magnitude of the Q-V shifts seen when channels are locked open or locked closed contains information about the coupling factor θ, which describes the energetic coupling between the voltage sensors and the channel gate. Ideally, we would want to measure the shift directly between the Q-V of fully closed channels and that of fully open channels, but these data were obtained from two different channel mutants. Although the G-V curves of wild type and the locked-closed mutant have similar $V_{1/2}$ values in the absence of Cd^{2+}, the G-V curves of the locked-open mutant were shifted more negative (Fig. S2), indicating that we cannot just directly compare the two Cd^{2+}-locked Q-V curves. Different parameters are needed to describe the gating behavior of the different mutants, but it is possible to model the relative effect of Cd^{2+} within each individual

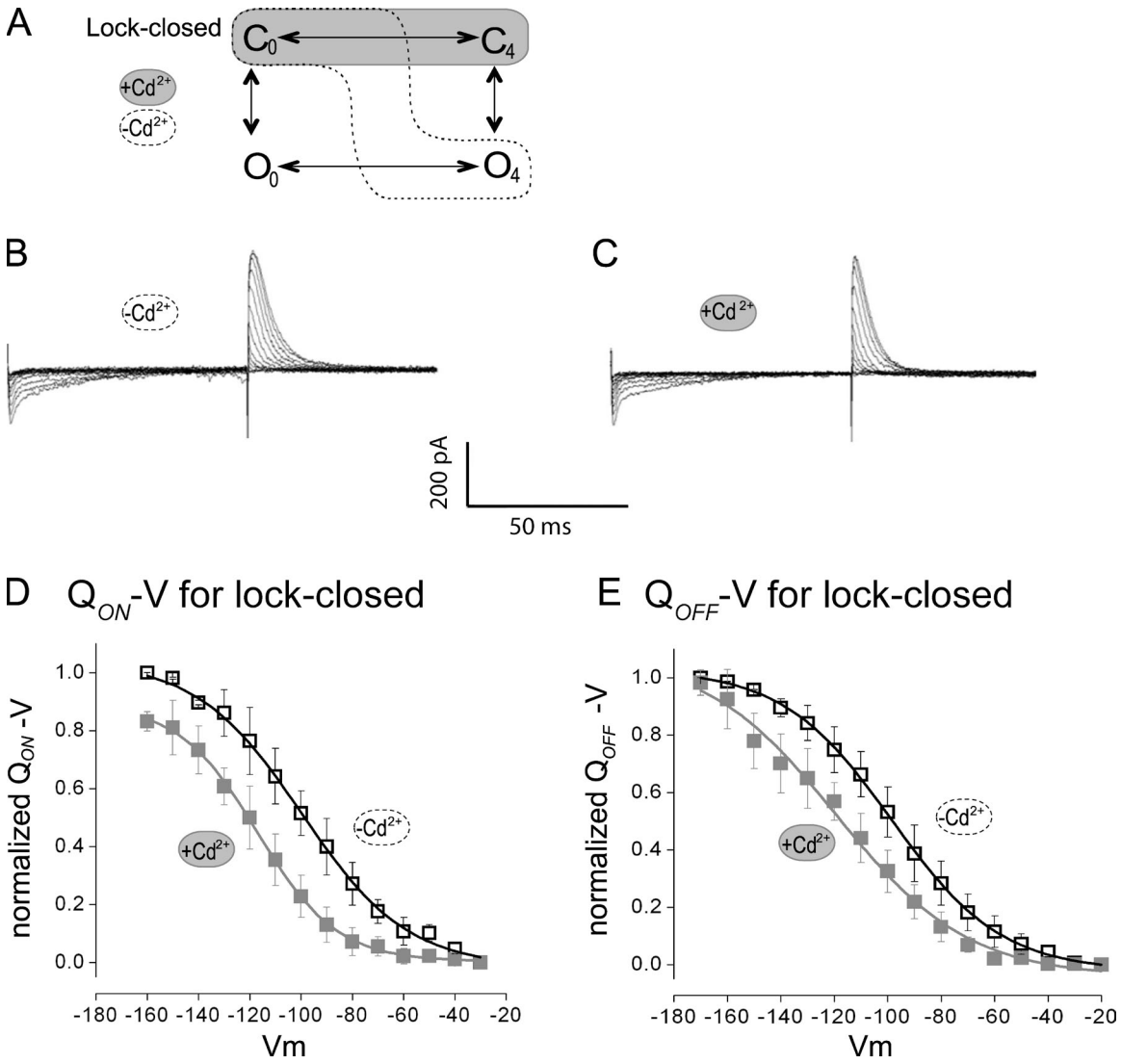

Figure 4. Gating current and Q-V relations for the spHCN 462Y468C mutant. (A) Schematic description of the locked-closed mutant. The state of the channel with Cd^{2+} is shaded, whereas the control condition without Cd^{2+} is in the dashed area. (B and C) Traces of gating current records for spHCN 462Y468C without (B) or with Cd^{2+} (C), from the same patch. Holding potential was 10 mV, and test pulses were from −30 to −170 mV in 10-mV increments. A −P/4 protocol was used to subtract leak and linear capacitive currents. (D and E) Normalized Q-V relations for spHCN 462Y468C without (open squares) or with Cd^{2+} (closed squares). Both Q_{ON} (D) and Q_{OFF} (E) were obtained by integrating components. Smooth curves are single Boltzmann fits to the data with these parameters as follows: Q_{ON} control: $V_{1/2}$ = −116.4 mV ± 8.4, slope factor (e-fold) = 21.2 ± 4.7; 100 µM cAMP + 130 nM free Cd^{2+}: $V_{1/2}$ = −131.8 ± 7.5 mV, slope factor(e-fold) = 18.1 ± 0.9; n = 5. Q_{OFF} control: $V_{1/2}$ = −96.7 ± 5.3 mV, slope factor (e-fold) = 16.0 ± 1.9; Cd^{2+}: $V_{1/2}$ = −128.0 ± 2.3 mV, slope factor (e-fold) = 21.1 ± 2.0; n = 7. Error bars represent SEM.

mutant using only the assumption that Cd^{2+} confines the conformational range of channel gating to open states (for the locked-open mutant) or to closed states (for the locked-closed mutant).

Fitting to a simple allosteric gating model reveals weak coupling between voltage sensor activation and channel opening

What is the relationship between voltage sensors and opening of the channel gate in the spHCN channel? Our observations seem to rule out an obligatory coupling between the two; for instance, if the channel can be open only when all the voltage sensors are activated, we would not have been able to observe voltage sensor charge movement in the locked-open channels. Instead, it seems likely, as hypothesized previously (Bruening-Wright et al., 2007), that the coupling between the voltage sensor and channel opening is allosteric, so that each activated voltage sensor makes channel opening more favorable.

To estimate the allosteric coupling coefficient θ, we fitted a general 10-state allosteric model of the voltage-dependent MWC scheme to our Q-V data as well as to G-V data on each mutant both with and without Cd^{2+}.

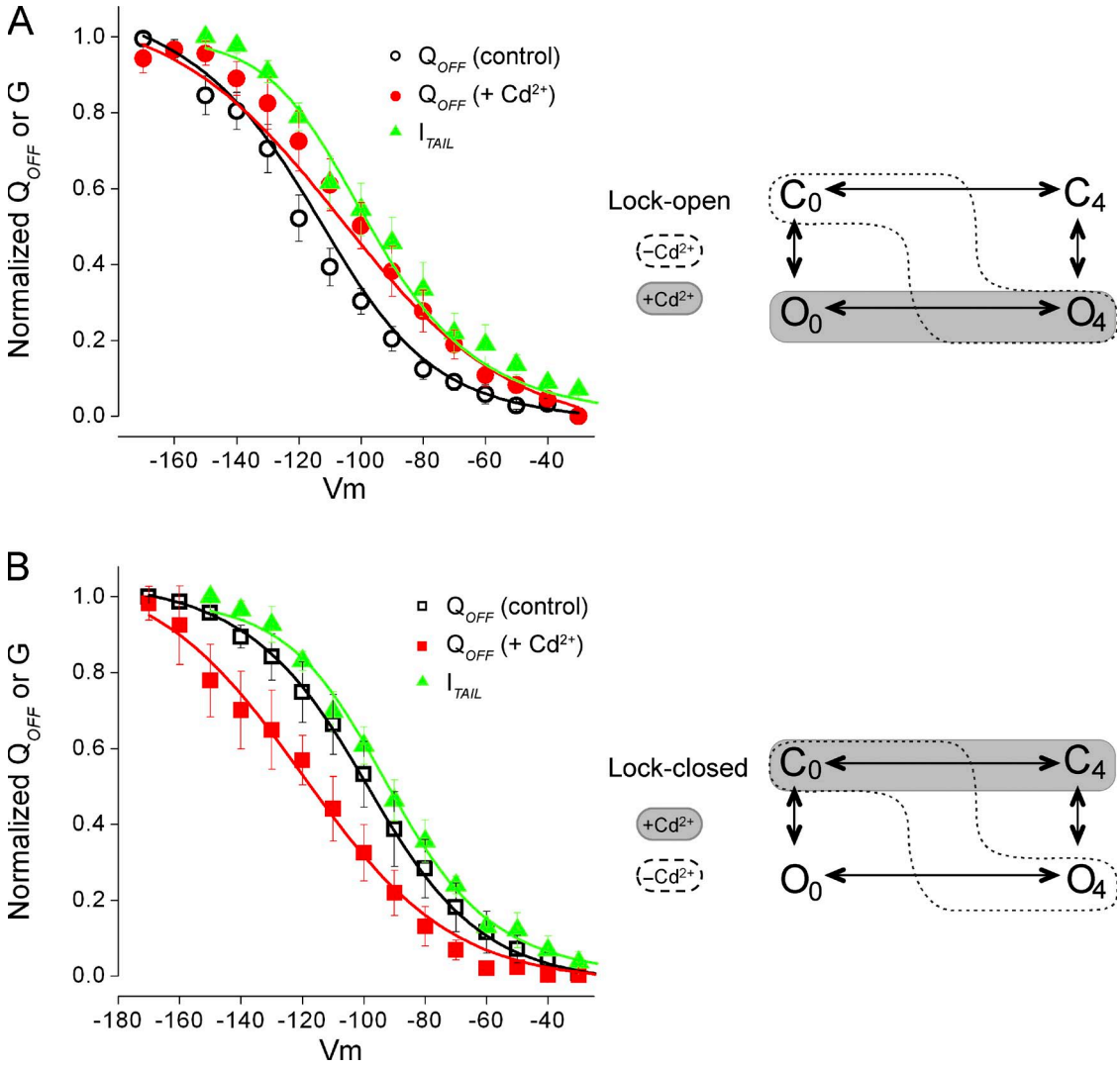

Figure 5. Comparison between the experimental Q-V and G-V characteristics of mutant channels and their respective fitting results with the 10-state allosteric model. (A) 462C466C; (B) 462Y468C. (A) Q-V (open and closed circles) and G-V (triangles) plots from spHCN 462C466C mutant channels (from Fig. 3 A), overlaid with the best fit from the 10-state model (black, red, and green lines; see parameter values in Table 2). (B) Q-V (open and closed squares) and G-V (triangles) plots recorded from 462Y468 mutant channels (from Fig. 4 A), overlaid with the best fit from the 10-state model (black, red, and green lines; see parameter values in Table 2). (A and B) The dotted outline shown in the simple four-state model on the right represents the states of the channel without Cd^{2+}, whereas the shaded outline represents the states of the channel with Cd^{2+}. Error bars represent SEM.

The 10-state allosteric model in the scheme (Fig. 1 A) is analogous to the models developed for BK channels (Horrigan et al., 1999) and KCNQ1 channels (Ma et al., 2011). Datasets for Q_{OFF} (Fig. 3 E and Fig. 4 E) were used, and to minimize any difference caused by the unusual ionic conditions, the G-V curves were measured under practically the same condition as the gating current experiments: 160 mM NMDG-methanesulfonate solution was constantly perfused during the test pulses (from −150 to −20 mV in 10-mV increments), and 160 mM K^+ was applied to the inside-out patches of the channels just before the switch to 60 mV. The resultant ionic tail current was used to compile G-V curves (Fig. 5, A and B).

The 10-state MWC model was used to fit the experimental results. There are only four parameters that control the equilibrium behavior of this model: $K_{gate(D)}$, the equilibrium constant between open and closed, when no voltage sensors are active; $K_{sens(C)}$, the equilibrium constant for voltage activation when the channel is closed; z, the gating charge associated with each voltage sensor's movement; and θ, the coupling factor. A previous study showed that including cooperativity did not improve the fit (Bruening-Wright et al., 2007), so we did not include any cooperativity between voltage sensors.

The MWC model is too simple to account for some known peculiarities of HCN channel gating—hysteresis, inactivation, and possibly multiple transitions in each S4 segment—but our experiments were designed to minimize the influence of these complex gating features. Hysteresis of the spHCN channel is observed

TABLE 1

Shifts in V_{median} and in $V_{1/2}$ occurring with Cd^{2+}

Parameter	V_{median}	$V_{1/2}$
462C466C Q_{ON} (0 mM Cd^{2+})	−117.9 ± 4.5	−132.7 ± 5.7
Q_{ON} (130 mM Cd^{2+})	−89.9 ± 10.3	−103.9 ± 8.9
Q_{OFF} (0 mM Cd^{2+})	−112.9 ± 3.2	−126.7 ± 4.2
Q_{OFF} (130 mM Cd^{2+})	−101.5 ± 4.4	−99.9 ± 5.4
462Y468C Q_{ON} (0 mM Cd^{2+})	−91.9 ± 8.4	−116.4 ± 4.8
Q_{ON} (130 mM Cd^{2+})	−104.8 ± 7.9	−131.8 ± 3.9
Q_{OFF} (0 mM Cd^{2+})	−94.7 ± 6.5	−96.7 ± 4.6
Q_{OFF} (130 mM Cd^{2+})	−106.6 ± 6.4	−128.0 ± 4.2

The trapezoid method (Chowdhury and Chanda, 2012) was used to calculate the V_{median} values from locked-open and locked-closed mutants, and $V_{1/2}$ values were calculated from a single Boltzmann fit.

when G-V or Q-V curves are measured from a prolonged stay at a hyperpolarizing holding potential compared with a depolarizing holding potential (Männikkö et al., 2005). Therefore, for the experimental conditions that require the observation of the shifts in Q-V curves by the application of Cd^{2+}, we designed the voltage protocol such that we held at depolarized potentials and measured the gating current during relatively brief hyperpolarizations (100 ms) to minimize the effect of hysteresis. We also used a saturating concentration of cAMP (100 µM), which abolishes the inactivation (Shin et al., 2004). Bruening-Wright et al. (2007) observed evidence for multiple S4 transitions in their voltage clamp fluorometry experiments. By focusing on steady-state Q-V curves for voltage sensor activation, our data should be little affected by the multiple steps, so long as they are sequential and together coupled to opening. Although the detailed shape (and the midpoint) of the Q-V curve might indeed be altered by multiple steps, we observed commensurate shifts in the median voltage for charge movement (Table 1), which has been shown by Chowdhury and Chanda (2012) to be directly related to the ΔG for full voltage-dependent excursion between closed and open states, independent of the details of the intervening steps.

For each mutant, we allowed a single set of MWC gating parameters to describe the data in both the absence and presence of Cd^{2+}; the effect of Cd^{2+} in the model was simply to restrict the channels to either open states (for the locked-open mutant) or closed states (for the locked-closed mutant). The fitting yielded well-constrained values for each gating parameter, with slight numerical differences between the two mutants (Fig. 5, A and B). From the fitting result, we estimate that the coupling between voltage sensors and channel gating for the two mutants is weak: the coupling constant θ was estimated to be 7.2 ± 3.0 fold per voltage sensor for the locked-open mutant and 3.6 ± 1.1 fold per voltage sensor for the locked-closed mutant (Table 2). Expressed in terms of molecular free energy change (kT ln θ), these values give an estimated coupling energy per voltage sensor of ∼1.3–2 kT.

TABLE 2

Parameters for curve fitting for Fig. 5

Parameter	462C466C (locked open)	462Y468C (locked closed)
$K_{gate(D)}$	0.26 ± 0.09	0.19 ± 0.15
θ	7.23 ± 3.04	3.56 ± 1.09
$K_{sens(C)}$	0.002 ± 0.001	0.007 ± 0.002
z	0.91 ± 0.05	1.03 ± 0.11

The coupling factor for spHCN seems quite weak in comparison to other voltage-gated channels. Several voltage-gated K^+ channels and Na^+ channels have been estimated to have extremely strict coupling between the voltage sensors and channel gates, with coupling factors of >100 per voltage sensor in *Shaker* and Kv2.1 channels (Islas and Sigworth, 1999), >50 per voltage sensor in voltage-gated Na^+ channels (Hirschberg et al., 1995), and >15 per voltage sensor in BK channels (Horrigan and Aldrich, 1999; Horrigan et al., 1999). Although structural and functional similarities exist between *Shaker* and HCN channels (Ledwell and Aldrich, 1999; Webster et al., 2004; Pathak et al., 2005) and the S4–S5 linker is involved in the coupling for both channels, the gate of the *Shaker* channel is very tightly coupled to gating charge movement such that the probability for voltage-independent opening is negligible, which is different from that of HCN channels. On the other hand, weaker coupling can be seen from some ligand-gated ion channels that open spontaneously (Ruiz and Karpen, 1997; Tibbs et al., 1997; Hui et al., 2003).

In summary, our data suggest that the gating behavior of spHCN channels can be accounted for by an allosteric scheme in which there is weak coupling between the voltage sensor transitions and the opening transition. In contrast to the highly refined and tightly coupled mechanism of depolarization-activated channels, the evolutionarily younger mechanism for hyperpolarization-activated channels seems to just barely suffice for effective voltage control of the channels. However, the weak voltage coupling may provide an advantage in that relatively small energetic contributions from modulatory influences (such as cyclic nucleotide binding or phosphorylation) can easily shift the voltage dependence of these channels.

We thank the members of the Yellen laboratory and Dr. Bruce Bean for their advice and suggestions and thank Tatiana Abramson for expert technical support.

This work was supported by a research grant (R01 HL070320) from the National Heart, Lung, and Blood Institute (National Institutes of Health) to G. Yellen.

Sharona E. Gordon served as editor.

Submitted: 22 June 2012
Accepted: 18 September 2012

REFERENCES

Altomare, C., A. Bucchi, E. Camatini, M. Baruscotti, C. Viscomi, A. Moroni, and D. DiFrancesco. 2001. Integrated allosteric model of voltage gating of HCN channels. *J. Gen. Physiol.* 117:519–532. http://dx.doi.org/10.1085/jgp.117.6.519

Beaumont, V., N. Zhong, R.C. Froemke, R.W. Ball, and R.S. Zucker. 2002. Temporal synaptic tagging by I(h) activation and actin: involvement in long-term facilitation and cAMP-induced synaptic enhancement. *Neuron.* 33:601–613. http://dx.doi.org/10.1016/S0896-6273(02)00581-0

Bell, D.C., H. Yao, R.C. Saenger, J.H. Riley, and S.A. Siegelbaum. 2004. Changes in local S4 environment provide a voltage-sensing mechanism for mammalian hyperpolarization-activated HCN channels. *J. Gen. Physiol.* 123:5–19. http://dx.doi.org/10.1085/jgp.200308918

Bezanilla, F., E. Perozo, D.M. Papazian, and E. Stefani. 1991. Molecular basis of gating charge immobilization in Shaker potassium channels. *Science.* 254:679–683. http://dx.doi.org/10.1126/science.1948047

Biel, M., C. Wahl-Schott, S. Michalakis, and X. Zong. 2009. Hyperpolarization-activated cation channels: from genes to function. *Physiol. Rev.* 89:847–885. http://dx.doi.org/10.1152/physrev.00029.2008

Bruening-Wright, A., F. Elinder, and H.P. Larsson. 2007. Kinetic relationship between the voltage sensor and the activation gate in spHCN channels. *J. Gen. Physiol.* 130:71–81. http://dx.doi.org/10.1085/jgp.200709769

Chen, S., J. Wang, and S.A. Siegelbaum. 2001. Properties of hyperpolarization-activated pacemaker current defined by coassembly of HCN1 and HCN2 subunits and basal modulation by cyclic nucleotide. *J. Gen. Physiol.* 117:491–504. http://dx.doi.org/10.1085/jgp.117.5.491

Chowdhury, S., and B. Chanda. 2012. Estimating the voltage-dependent free energy change of ion channels using the median voltage for activation. *J. Gen. Physiol.* 139:3–17. http://dx.doi.org/10.1085/jgp.201110722

Cox, D.H., J. Cui, and R.W. Aldrich. 1997. Separation of gating properties from permeation and block in *mslo* large conductance Ca-activated K^+ channels. *J. Gen. Physiol.* 109:633–646. http://dx.doi.org/10.1085/jgp.109.5.633

Dekker, J.P., and G. Yellen. 2006. Cooperative gating between single HCN pacemaker channels. *J. Gen. Physiol.* 128:561–567. http://dx.doi.org/10.1085/jgp.200609599

Demontis, G.C., B. Longoni, U. Barcaro, and L. Cervetto. 1999. Properties and functional roles of hyperpolarization-gated currents in guinea-pig retinal rods. *J. Physiol.* 515:813–828. http://dx.doi.org/10.1111/j.1469-7793.1999.813ab.x

DiFrancesco, D. 1993. Pacemaker mechanisms in cardiac tissue. *Annu. Rev. Physiol.* 55:455–472. http://dx.doi.org/10.1146/annurev.ph.55.030193.002323

Gauss, R., R. Seifert, and U.B. Kaupp. 1998. Molecular identification of a hyperpolarization-activated channel in sea urchin sperm. *Nature.* 393:583–587. http://dx.doi.org/10.1038/31248

Hilgemann, D.W. 1989. Giant excised cardiac sarcolemmal membrane patches: sodium and sodium-calcium exchange currents. *Pflugers Arch.* 415:247–249. http://dx.doi.org/10.1007/BF00370601

Hirschberg, B., A. Rovner, M. Lieberman, and J. Patlak. 1995. Transfer of twelve charges is needed to open skeletal muscle Na^+ channels. *J. Gen. Physiol.* 106:1053–1068. http://dx.doi.org/10.1085/jgp.106.6.1053

Horrigan, F.T., and R.W. Aldrich. 1999. Allosteric voltage gating of potassium channels II. Mslo channel gating charge movement in the absence of Ca^{2+}. *J. Gen. Physiol.* 114:305–336. http://dx.doi.org/10.1085/jgp.114.2.305

Horrigan, F.T., J. Cui, and R.W. Aldrich. 1999. Allosteric voltage gating of potassium channels I. Mslo ionic currents in the absence of Ca^{2+}. *J. Gen. Physiol.* 114:277–304. http://dx.doi.org/10.1085/jgp.114.2.277

Hui, K., B. Liu, and F. Qin. 2003. Capsaicin activation of the pain receptor, VR1: multiple open states from both partial and full binding. *Biophys. J.* 84:2957–2968. http://dx.doi.org/10.1016/S0006-3495(03)70022-8

Ishii, T.M., M. Takano, L.H. Xie, A. Noma, and H. Ohmori. 1999. Molecular characterization of the hyperpolarization-activated cation channel in rabbit heart sinoatrial node. *J. Biol. Chem.* 274:12835–12839. http://dx.doi.org/10.1074/jbc.274.18.12835

Islas, L.D., and F.J. Sigworth. 1999. Voltage sensitivity and gating charge in *Shaker* and *Shab* family potassium channels. *J. Gen. Physiol.* 114:723–742. http://dx.doi.org/10.1085/jgp.114.5.723

Kaupp, U.B., and R. Seifert. 2001. Molecular diversity of pacemaker ion channels. *Annu. Rev. Physiol.* 63:235–257. http://dx.doi.org/10.1146/annurev.physiol.63.1.235

Ledwell, J.L., and R.W. Aldrich. 1999. Mutations in the S4 region isolate the final voltage-dependent cooperative step in potassium channel activation. *J. Gen. Physiol.* 113:389–414. http://dx.doi.org/10.1085/jgp.113.3.389

Liu, Y., M. Holmgren, M.E. Jurman, and G. Yellen. 1997. Gated access to the pore of a voltage-dependent K^+ channel. *Neuron.* 19:175–184. http://dx.doi.org/10.1016/S0896-6273(00)80357-8

Ludwig, A., X. Zong, M. Jeglitsch, F. Hofmann, and M. Biel. 1998. A family of hyperpolarization-activated mammalian cation channels. *Nature.* 393:587–591. http://dx.doi.org/10.1038/31255

Ma, L.-J., I. Ohmert, and V. Vardanyan. 2011. Allosteric features of KCNQ1 gating revealed by alanine scanning mutagenesis. *Biophys. J.* 100:885–894. http://dx.doi.org/10.1016/j.bpj.2010.12.3726

Magee, J.C. 1999. Dendritic I_h normalizes temporal summation in hippocampal CA1 neurons. *Nat. Neurosci.* 2:508–514. http://dx.doi.org/10.1038/9158

Männikkö, R., F. Elinder, and H.P. Larsson. 2002. Voltage-sensing mechanism is conserved among ion channels gated by opposite voltages. *Nature.* 419:837–841. http://dx.doi.org/10.1038/nature01038

Männikkö, R., S. Pandey, H.P. Larsson, and F. Elinder. 2005. Hysteresis in the voltage dependence of HCN channels: conversion between two modes affects pacemaker properties. *J. Gen. Physiol.* 125:305–326. http://dx.doi.org/10.1085/jgp.200409130

McCormick, D.A., and H.C. Pape. 1990. Properties of a hyperpolarization-activated cation current and its role in rhythmic oscillation in thalamic relay neurones. *J. Physiol.* 431:291–318.

Monod, J., J. Wyman, and J.P. Changeux. 1965. On the nature of allosteric transitions: a plausible model. *J. Mol. Biol.* 12:88–118. http://dx.doi.org/10.1016/S0022-2836(65)80285-6

Pathak, M., L. Kurtz, F. Tombola, and E. Isacoff. 2005. The cooperative voltage sensor motion that gates a potassium channel. *J. Gen. Physiol.* 125:57–69. http://dx.doi.org/10.1085/jgp.200409197

Proenza, C., and G. Yellen. 2006. Distinct populations of HCN pacemaker channels produce voltage-dependent and voltage-independent currents. *J. Gen. Physiol.* 127:183–190. http://dx.doi.org/10.1085/jgp.200509389

Rothberg, B.S., K.S. Shin, P.S. Phale, and G. Yellen. 2002. Voltage-controlled gating at the intracellular entrance to a hyperpolarization-activated cation channel. *J. Gen. Physiol.* 119:83–91. http://dx.doi.org/10.1085/jgp.119.1.83

Rothberg, B.S., K.S. Shin, and G. Yellen. 2003. Movements near the gate of a hyperpolarization-activated cation channel. *J. Gen. Physiol.* 122:501–510. http://dx.doi.org/10.1085/jgp.200308928

Ruiz, M.L., and J.W. Karpen. 1997. Single cyclic nucleotide-gated channels locked in different ligand-bound states. *Nature.* 389:389–392. http://dx.doi.org/10.1038/38744

Santoro, B., S.G. Grant, D. Bartsch, and E.R. Kandel. 1997. Interactive cloning with the SH3 domain of N-src identifies a new brain specific ion channel protein, with homology to eag and cyclic nucleotide-gated channels. *Proc. Natl. Acad. Sci. USA.* 94:14815–14820. http://dx.doi.org/10.1073/pnas.94.26.14815

Santoro, B., D.T. Liu, H. Yao, D. Bartsch, E.R. Kandel, S.A. Siegelbaum, and G.R. Tibbs. 1998. Identification of a gene encoding a hyperpolarization-activated pacemaker channel of brain. *Cell.* 93:717–729. http://dx.doi.org/10.1016/S0092-8674(00)81434-8

Sesti, F., S. Rajan, R. Gonzalez-Colaso, N. Nikolaeva, and S.A. Goldstein. 2003. Hyperpolarization moves S4 sensors inward to open MVP, a methanococcal voltage-gated potassium channel. *Nat. Neurosci.* 6:353–361. http://dx.doi.org/10.1038/nn1028

Shin, K.S., C. Maertens, C. Proenza, B.S. Rothberg, and G. Yellen. 2004. Inactivation in HCN channels results from reclosure of the activation gate: desensitization to voltage. *Neuron.* 41:737–744. http://dx.doi.org/10.1016/S0896-6273(04)00083-2

Tibbs, G.R., E.H. Goulding, and S.A. Siegelbaum. 1997. Allosteric activation and tuning of ligand efficacy in cyclic-nucleotide-gated channels. *Nature.* 386:612–615. http://dx.doi.org/10.1038/386612a0

Wang, J., S. Chen, M.F. Nolan, and S.A. Siegelbaum. 2002. Activity-dependent regulation of HCN pacemaker channels by cyclic AMP: signaling through dynamic allosteric coupling. *Neuron.* 36:451–461. http://dx.doi.org/10.1016/S0896-6273(02)00968-6

Webster, S.M., D. Del Camino, J.P. Dekker, and G. Yellen. 2004. Intracellular gate opening in Shaker K+ channels defined by high-affinity metal bridges. *Nature.* 428:864–868. http://dx.doi.org/10.1038/nature02468